OPEN ACCESS

GAVIN PUBLISHERS

Current Research in Clinical Diabetes and Obesity

Paszkiewicz RL, et al. Curr Res Clin Diab Obes 1: 102.

Research Article

DOI: 10.29011/CRCDO-102.100002

EndoBarrier® Implantation Results in Fecalization of the Small Bowel Microbiome and Inflammation in a Canine Model

Rebecca L. Paszkiewicz[1#], Gabriela Leite[2#], Walter Morales[2], Stacy Weitsman[2], Gillian M. Barlow[2], Mark Pimentel[2,3], Miguel A. Burch[4], Hasmik Mkrtchyan[5], Marilyn Ader[5], Richard N. Bergman[5], Ruchi Mathur[2,6*]

[1]Pediatric Endocrinology, University of California, Los Angeles, CA, USA

[2]Medically Associated Science and Technology (MAST) Program, Cedars-Sinai Medical Center, Los Angeles, CA, USA

[3]Division of Digestive and Liver Diseases, Cedars-Sinai Medical Center, Los Angeles, CA, USA

[4]Minimally Invasive and GI Surgery, Cedars-Sinai Medical Center, Los Angeles, CA, USA

[5]Diabetes and Obesity Research Institute, Cedars-Sinai Medical Center, Los Angeles, CA, USA

[6]Division of Endocrinology, Diabetes and Metabolism, Cedars-Sinai Medical Center, Los Angeles, Los Angeles, CA, USA

[#]RLP and GL contributed equally to this manuscript and are co-first authors

[*]**Corresponding author:** Ruchi Mathur, Director, Clinical Diabetes, Cedars-Sinai Medical Center, 8700 Beverly Blvd, Becker 131, Los Angeles, California 90048, USA

Citation: Paszkiewicz RL, Leite G, Morales W, Weitsman S, Barlow GM, et al. (2020) EndoBarrier® Implantation Results in Fecalization of the Small Bowel Microbiome and Inflammation in a Canine Model. Curr Res Clin Diab Obes 1: 102. DOI: 10.29011/CRCDO-102.100002

Received Date: 17 February, 2019; **Accepted Date:** 04 March, 2020; **Published Date:** 09 March, 2020

Abstract

The EndoBarrier® is an endoluminal duodenal-jejunal bypass liner that aids weight loss by forming a barrier between ingested nutrients and the small intestinal surface. However, the device safety has been questioned. We investigated EndoBarrier® effects on the duodenal microbiome and inflammatory responses using a canine model. Male mongrel dogs (N=7) were implanted with EndoBarriers® for 7 weeks. Duodenal microbiome profiles and circulating cytokine levels were compared at implantation and explantation. Normal fecal microbiome profiles were determined in unimplanted controls (N=3). The duodenal microbiome at explantation differed significantly from implantation, and had shifted to a microbial profile closer to that of the normal fecal microbiome. Relative abundance of phylum Proteobacteria in the duodenum was decreased 54.76-fold, with increases in Fusobacteria, Firmicutes and Bacteroidetes. At the family level, relative abundances of Enterobacteriaceae and Desulfovibrionaceae (phylum Proteobacteria) in the duodenum were significantly decreased at explantation (FC=65.42, FDR P-value=1.72E-4; and FC=38.31, FDR P-value=9.93E-8, respectively), and Lactobacillaceae and Clostridiaceae (phylum Firmicutes) and Fusobacteriaceae (phylum Fusobacteria) were increased. Cytokine levels (IL2, IL6, IL18, GM-CSF, and TNFα) were significantly increased at implantation week 3 and at explantation, and IL2 and GM-CSF remained elevated 6 weeks after EndoBarrier® removal. These findings indicate that EndoBarrier® implantation is associated with significant changes in the duodenal microbiome, and with inflammatory perturbations that persist after removal, and thus have implications for its clinical use.

Introduction

The incidence and prevalence of both obesity and diabetes have reached pandemic levels [1-3], and reducing the burden of these diseases is a primary focus of research. Surgical interventions such as gastric bypass have shown benefits in weight loss and improved glucose profiles [4], but are costly and invasive. The EndoBarrier® (GI Dynamics Inc., Lexington, MA) is an endoluminal Duodenal-Jejunal Bypass Liner (DJBL) that provides a mechanical barrier

between ingested nutrients and the absorptive surface of the small intestine [5]. It is open at both ends, promoting the passage of gastric juices and nutrients from the stomach to the jejunum, mimicking a gastric bypass. Normally secreted pancreatic juices and bile will enter the duodenum but remain on the outside of the sleeve and do not come in contact with the luminal contents [5]. Although the EndoBarrier® has benefits in weight loss [5,6], its safety has been questioned and in 2015, enrollment in a pivotal U.S. trial ceased on the recommendation of the independent data and safety monitoring board when seven cases of liver abscesses were reported (a 3.5% incidence) [7].

The gut microbiome is known to significantly influence weight gain and metabolism in the host [8-11], and perturbations of the gut microbiome have been described both in obesity [12-15] and in type 2 diabetes [16,17]. A recent study by de Jonge et al. demonstrated that human subjects with obesity exhibit changes in the gut microbiome following EndoBarrier® placement, which may contribute to the weight loss and metabolic improvements in these subjects [18]. However, these studies were performed using stool samples, which are not representative of the entire gastrointestinal tract. The small bowel is central to the processes of digestion and absorption, and contains microbes that enable the host to utilize otherwise indigestible carbohydrates and host-derived glycoconjugates, among other functions [19-22]. As such, examining the direct effects of EndoBarrier® implantation on the small bowel microbiome is of tremendous clinical importance.

We have previously used a canine model to explore the metabolic effects of EndoBarrier® implantation [23,24], as the use of an animal model allows more invasive and comprehensive studies than can be performed using human subjects. Dogs are an ideal model of human obesity as, when fed a diet supplemented with a moderate amount of fat (similar to a fast-food diet), they gain weight to a degree that is comparable to most humans, and also gain similar amounts of both subcutaneous and abdominal fat. Moreover, the duodenum in these animals is similar in size to the human duodenum, and as such the Endobarrier® (which is designed for human use) can be successfully implanted. In this study, we used this canine model to explore for the first time the effects of the EndoBarrier® on the small intestinal microbiome, and on systemic inflammatory responses, during EndoBarrier® implantation and following its explantation.

Materials and Methods

Animals and Study Design

Male mongrel dogs (N=7) aged 12-14 months and weighing 28.6±1.2 kg at baseline were used in this study. None of the animals had undergone any previous interventions. Before starting the study, animals were cleared as having good bills of health by veterinary staff. All experiments were conducted in conformity with the Public Health Service Policy on Humane Care and Use of Laboratory Animals, and were approved by the Cedars-Sinai Medical Center Institutional Animal Care and Use Committee (IACUC).

All animals were housed in individual runs in the vivarium, under a 12:12 hours light/dark cycle. Animals were given free access to water, and were fed daily from 9 am to 1 pm with the normal study diet composed of 415 g of Hill's Prescription Diet (Hill's Pet Nutrition, Topeka, KA) (10% carbohydrate, 9% protein, 8% fat, 0.3% fiber, and 73% moisture) and 825 g of Laboratory HDL Canine Diet and Prolab Canine 2000 (LabDiet, Hayward, CA) (40% carbohydrate, 26% protein, 14% fat, and 3% fiber).

EndoBarrier® Implantation and Removal

The proximal end of the EndoBarrier® liner consists of barbed nitinol anchors which allow the device to attach to the duodenal bulb during an endoscopic procedure. For EndoBarrier® implantation, dogs (N=7) were sedated with a subcutaneous injection of acepromazine (0.1mg/kg), and then Propofol (3 mg/kg) was injected intravenously into a cephalic vein. Dogs were intubated and inhaled isoflurane (3%) was used to maintain a stable level of anesthesia. The small intestine was accessed through a standard endoscope (Karl Storz, El Segundo, CA), and the EndoBarrier® was placed in the duodenum as described previously [25]. After confirmation of full deployment of the liner, dogs were returned to the vivarium and monitored for recovery from anesthesia. For up to 3 days after implantation, dogs were fed a soft diet (Hill's Prescription Diet) before returning to the normal study diet described above.

EndoBarriers® were removed at week 7-8, with induction and maintenance of anesthesia as described above. An endoscope was used to visualize drawstrings attached to the nitinol anchor. The retrieval hood was used to collapse and capture the anchor, and the endoscope, retrieval grasper, and implant were all removed together. Dogs were then returned to the vivarium to recover from the anesthesia, and were fed a soft diet (Hill's Prescription Diet) for up to 3 days before returning to the normal study diet.

Blood Collection and Quantification of Plasma Inflammatory Markers

After an overnight fast, blood samples were collected from the lower front leg (cephalic vein) using a single needlestick (17G; PHS, Temecula, CA) into 1.7 mL tubes containing EDTA and heparin. Samples were centrifuged and plasma was stored at -80˚C. Levels of inflammatory markers were simultaneously detected and quantified using a multiplex magnetic bead-based immunoassay using FlexMAP 3D® technology (Luminex, Austin, TX, USA) and the Canine Cytokine Magnetic Bead Panel (CCYTOMAG-90K, EMD Millipore Corporation, Billerica, MA). Data were acquired using FlexMAP 3D system (Luminex), considering a minimum

of 50 events per bead, gate setting 8,000 to 15,000 and default reporter gain (low PMT). The assay allowed the detection of cytokine concentrations from 12.2 pg/ml to 50,000 pg/ml. One extra dilution point on the standard curve was added, extending the lower limit of detection to 3.05 pg/ml. For INFγ, the assay allowed the detection of concentrations from 2.44 pg/ml to 10,000 pg/ml. One extra dilution point on the standard curve was added, extending the lower limit to 0.61 pg/ml.

Aspirate and Stool Sample Collection and DNA Extraction

Luminal samples from the duodenum were collected through the endoscope immediately prior to EndoBarrier® placement and after its removal, using sterile saline to flush the duodenum. Samples were collected into sterile tubes and stored at -80°C. Aspirates were thawed on ice, treated with 1:1 1x Sputolysin (Millipore) and vortexed until fully liquefied, and DNA extractions were performed using the MagAttract PowerSoil DNA KF Kit (Qiagen) as described previously [26]. Duodenal sampling was performed on the day of EndoBarrier® implantation and on the day of removal (explantation). Stool samples were collected from control dogs (N=3) that were housed and fed under the same conditions as the EndoBarrier®-implanted animals, but which were not part of the study. Stool samples were placed on ice and transported immediately to the laboratory, and DNA extractions were performed as described above.

16S Library Preparation and Metagenomic Sequencing

The preparation of 16S libraries from duodenal aspirate and stool samples was carried out following the Illumina protocol available at http://sapac.support.illumina.com/downloads/16s_metagenomic_sequencing_library_preparation.html, with modifications as described previously [26]. The V3 and V4 regions were amplified using the published gene-specific primers S-D-Bact-0341-b-S-17 and S-D-Bact-0785-a-A-21 [27]. The Clean-Up step was also optimized using a previously described modification [28], and performed using Agencourt AMPure XP beads as described previously [26]. V3 and V4 libraries from duodenal aspirate and stool samples were sequenced using the MiSeq Reagent Kit v3 (600-cycles) on a MiSeq System (Illumina). 2x301 cycles of paired-end sequencing were performed per the manufacturer's protocol, and 15% Phix (Illumina) was added to each library pool. Samples that generated less than 2,000 reads were excluded from the analysis. Sequencing analysis was performed as described previously [26].

Statistical Analysis for Plasma Inflammatory Markers

Luminex data were analyzed using xPonent v3.1 software (Luminex). Median Fluorescent Intensity (MFI) data analysis was performed using a five-parameter logistic regression curve derived from the standard curve. Since one extra standard point was added to the test, samples below the lower limit of quantitation were designated as undetected. Metabolic pathway analysis was carried out using Ingenuity Pathway Analysis software (Qiagen, Valencia, CA, USA). Statistical paired T-tests, Mann-Whitney tests and graph construction were performed using GraphPad Prism 7.02 (GraphPad Software, La Jolla, CA, USA).

Data Availability

The datasets generated during the current study are available at the National Center for Biotechnology Information (NCBI) Bio Project Repository https://www.ncbi.nlm.nih.gov/bioproject under BioProject ID PRJNA590520.

Results

Experimental Animals and Microbiome Samples

Experimental animals were male mongrel dogs (N=7) aged 12-14 months old at baseline, and weighing 23.2-32.6 kg. All were naïve of treatment, and were cleared as having good bills of health by veterinary staff prior to beginning any experiments. Samples of the duodenal microbiome were obtained from 5/7 dogs during EndoBarrier® implantation, and from the same 5 dogs again 7 weeks later at EndoBarrier® explantation. One of the explantation samples was excluded from the final analysis as it generated less than 2,000 sequencing reads. The normal control fecal microbiome was analyzed using stool samples from 3 dogs which were housed and fed in the same facility under the same conditions, but which did not undergo EndoBarrier® implantation.

Microbiome Analysis

16S rRNA gene sequencing revealed significant differences between the duodenal microbiome at EndoBarrier® implantation and by the time of device explantation 7 weeks later. Beta-diversity analysis demonstrated that the duodenal microbiome at explantation was significantly altered from that at implantation (P=0.0159, Figure 1), and demonstrated greater similarity to the normal fecal microbiome in control dogs (P=0.1429, Figure 1). Hierarchical clustering confirmed that the duodenal microbiome at explantation exhibited differences in more than 200 Operational Taxonomic Units (OTUs) when compared to the duodenal microbiome at implantation, and showed many similarities to the normal fecal microbiome from control dogs (Figure 2).

At the phylum level, the canine duodenal microbiome at implantation was characterized by a high relative abundance of Proteobacteria (~75%), with lower levels of Bacteroidetes (~10%), Firmicutes (~10%) and other phyla (Figure 3). By the time of EndoBarrier® explantation, the duodenal microbiome had shifted to a profile characterized by a higher relative abundance of phylum Fusobacteria (~37%), followed by Firmicutes (~29%) and Bacteroidetes (~25%). In comparison, the normal fecal microbiome of control dogs was characterized by a high relative abundance of Firmicutes (~55%), followed by Bacteroidetes (~23%) and Fusobacteria (~19%) (Figure 3).

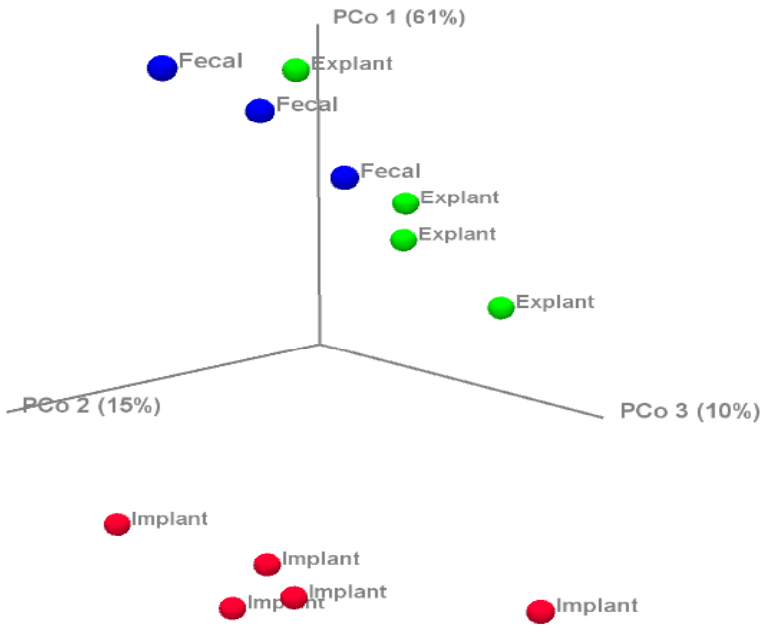

Figure 1: Principal Coordinates Analysis plot of binary and abundance-weighted UniFrac distances of the duodenal microbiome of dogs at EndoBarrier® implantation (N=5, shown in red) and at EndoBarrier® explantation (N=4, shown in green), and of the fecal microbiome of control dogs (N=3, shown in blue).

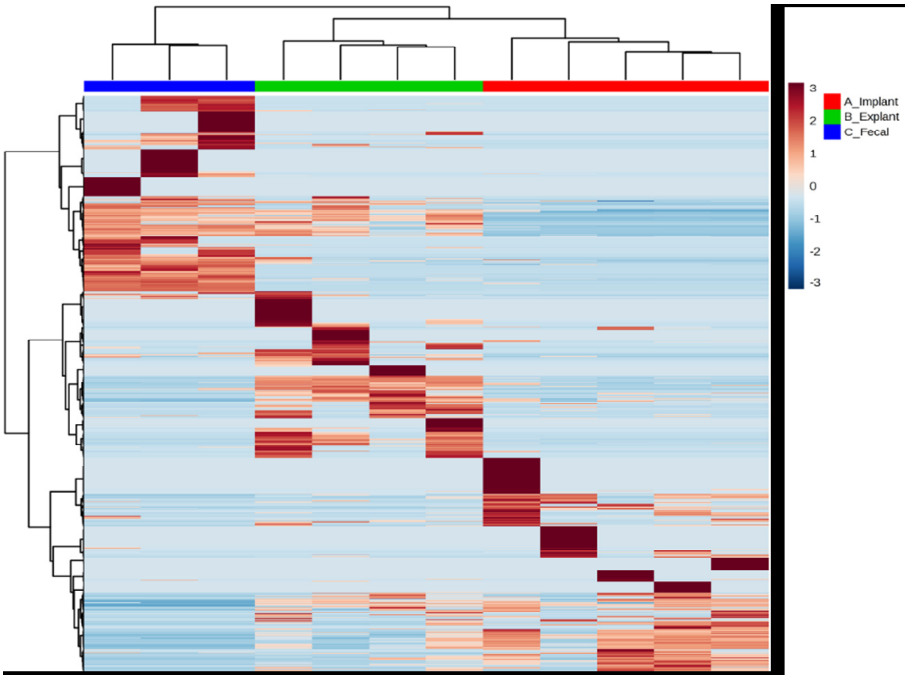

Figure 2: Hierarchical clustering of all dogs included in this study based on the microbiome profiles of duodenal aspirates at EndoBarrier® implantation (shown in red) and at EndoBarrier® explantation (shown in green), and of the fecal microbiome of control dogs (shown in blue).

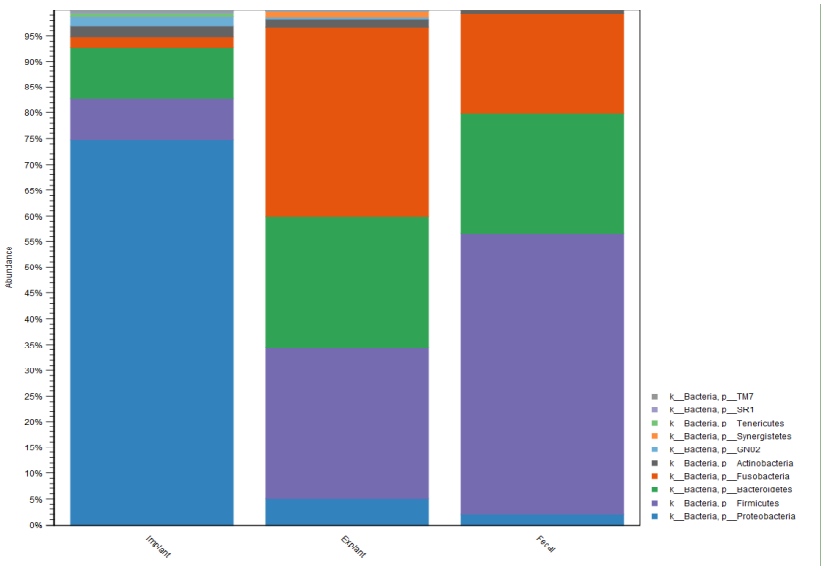

Figure 3: Relative abundances of bacterial phyla in the duodenal microbiome at EndoBarrier® implantation (left) and at EndoBarrier® explantation (middle), and in the fecal microbiome of control dogs (right).

Alterations in the Phylum Proteobacteria

At the time of EndoBarrier® explantation, the relative abundance of the phylum Proteobacteria was decreased 54.76-fold compared to that at implantation (FDR P-value=5.15E-7), and was characterized by bacteria from the families Enterobacteriaceae (FC=65.42, FDR P-value=1.72E-4) and Desulfovibrionaceae (FC=38.31, FDR P-value=9.93E-8) (Figure 4). When compared to the normal fecal microbiome of control dogs, there was no statistical difference between the relative abundance of family Enterobacteriaceae in the duodenal microbiome at EndoBarrier® explantation and the normal fecal microbiome (FC=0.5, FDR P-value=0.93). In contrast, the relative abundance of the family Desulfovibrionaceae was increased in the duodenal microbiome at EndoBarrier® explantation compared to the normal fecal microbiome (FC=3464, FDR P-value=1.64E-4), and some members of this family were absent from the control fecal microbiome.

Figure 4: Sunburst representations illustrating differences in phylum Proteobacteria in the duodenal microbiome at EndoBarrier® implantation (left) and at EndoBarrier® explantation (right). Differences in the family Desulfovibrionaceae are highlighted.

Alterations in the Phylum Fusobacteria

The relative abundance of phylum Fusobacteria, which represented only 2% of the total microbial content in duodenal samples at implantation, was increased 11-fold at the time of EndoBarrier® explantation (FDR P-value=1.50E-4), and was now primarily represented by the family Fusobacteriaceae (99%) (Figure S1), which had increased 28-fold compared to implantation (FDR P-value<0.0001). The same Fusobacterial profile was observed in the control fecal microbiome (Figure S1), and there were no statistically significant differences between the Fusobacterial profiles in the duodenal microbiome at explantation and in the control fecal microbiome (FDR P-value=0.58). In contrast, phylum Fusobacteria in the duodenum at implantation also included several genera from the family Leptotrichiaceae (15%), which were not seen at explantation (Figure S1).

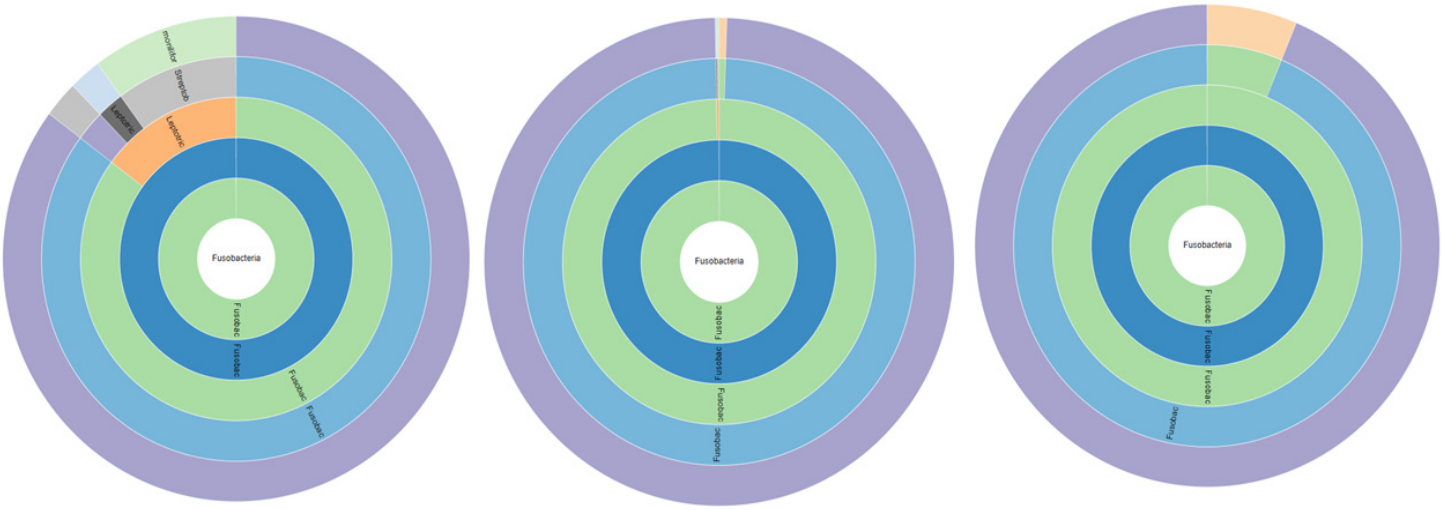

Figure S1: Sunburst representations illustrating differences in phylum Fusobacteria in the duodenal microbiome at EndoBarrier® implantation (left) and at EndoBarrier® explantation (middle), and in the fecal microbiome of control dogs (right).

Alterations in the Phylum Firmicutes

At EndoBarrier® explantation, the phylum Firmicutes had shifted to a profile more similar to that of the control fecal microbiome, which was characterized by high relative abundances of the families Lactobacillaceae (~42%) and Clostridiaceae (~20%) (Figure 5). These two families were significantly increased in the duodenal microbiome at explantation when compared to that at implantation (FC=87.71, FDR P-value=1.02E-6 and FC=70.78, FDR P-value=1.25E-5, respectively). Specific genera from these families, comprising mostly facultative and obligative anaerobes, were also significantly increased in the duodenal microbiome at explantation, including *Lactobacillus* (FC=117.42, FDR P-value=7.89E-7) and *Clostridium* (FC=148.05, FDR P-value=1.07E-6). In contrast, the family Aerococcaceae (which has a majority of aerobic species) was highly represented in the duodenal microbiome at EndoBarrier® implantation, and was found to have significantly decreased at explantation (FC=-27.12, FDR P-value=2.69E-4) (Figure 5).

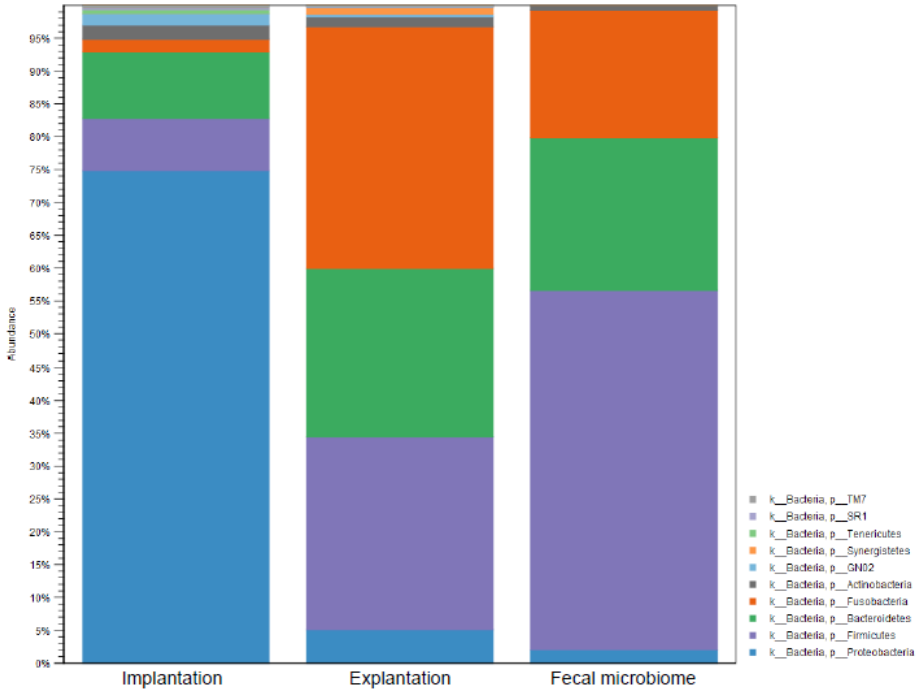

Figure 5: Area chart representation of the differences in phylum Firmicutes in the duodenal microbiome at EndoBarrier® implantation (left) and at EndoBarrier® explantation (middle), and in the fecal microbiome of control dogs (right).

Markers of Inflammation

Fasting blood samples obtained from all 7 dogs at baseline, at week 3 of the EndoBarrier® implantation period, at EndoBarrier® removal, and at week 6 after EndoBarrier® explantation were used to measure plasma levels of the pro- and anti-inflammatory cytokines and chemokines monocyte chemoattractant protein 1 (MCP1), interferon gamma (IFNγ), interleukin 2 (IL2), interleukin 6 (IL6), interleukin 7 (IL7), interleukin 8 (IL8), interleukin 10 (IL10), interleukin 18 (IL18), granulocyte-macrophage colony-stimulating factor (GM-CSF), and tumor necrosis factor alpha (TNFα).

As shown in Table 1, levels of the pro-inflammatory cytokines and chemokines IL2, IL6, IL18, GM-CSF, and TNFα were significantly increased at week 3 of implantation (FC=24.44, P=0.0156; FC=7.46, P=0.0313; FC=6.08, P=0.0156; FC=32.37, P=0.0156; FC=8.14, P=0.0313; respectively) and at EndoBarrier® explantation (FC=3.78, P=0.0156; FC=3.2, P=0.0156; FC=3.69, P=0.0156; FC=8.68, P=0.0156; FC=2.59, P=0.0156; respectively) when compared to baseline. Levels of IL-7, which can be both pro- and anti-inflammatory, particularly in the gut [29], were increased at week 3 of implantation (FC=45.74, P=0.0313) and at EndoBarrier® explantation (FC=8.29, P=0.0156) compared to baseline. In contrast, levels of the anti-inflammatory marker IL10 did not change during the EndoBarrier® implantation period. At week 6 following EndoBarrier® removal, all previously elevated markers of inflammation had returned to baseline levels with the exception of IL2 and GM-CSF, which remained elevated (FC=6.83, P=0.0469 and FC=8.5, P=0.0313, respectively).

	Week 3 of EndoBarrier® implantation period		EndoBarrier® explantation		Week 6 after EndoBarrier® explantation	
	Fold change	P-value	Fold change	P-value	Fold change	P-value
IL18	6.08	1.56E-02	3.69	1.56E-02	4.13	ns
IFNγ	1.23	ns	1.38	ns	1.46	ns
IL2	24.44	1.56E-02	3.78	1.56E-02	6.83	4.69E-02

IL6	7.46	3.13E-02	3.2	1.56E-02	3.27	ns
IL8	5.83	ns	1.14	ns	4.35	ns
IL10	36.69	ns	3.44	ns	20.6	ns
MCP1	2.52	ns	2.11	ns	-1.03	ns
TNFα	8.14	3.13E-02	2.59	1.56E-02	3.56	ns
IL7	45.74	3.13E-02	8.29	1.56E-02	5.16	ns
GM-CSF	32.37	1.56E-02	8.68	1.56E-02	8.5	3.13E-02

Wilcoxon paired test, ns – no statistical significance.

Table 1: Change in the levels of systemic markers of inflammation at week 3 of EndoBarrier® implantation, at EndoBarrier® removal, and at week 6 after EndoBarrier® explantation. The values represent the fold change from levels at baseline.

Inflammatory Pathways Altered in Response to Endobarrier® Placement

IPA analysis predicts the downstream effects on biological processes based on the expression state of each target included in the analysis. The results revealed that the inflammatory markers analyzed at week 3 of EndoBarrier® implantation exhibited a pattern consistent with inflammatory responses to bacterial lipopolysaccharide (Z-score=2.363, FDR P-value=2.85E-12) and to peptidoglycan (Z-score=2.119, FDR P-value=2.03E-11), which were the two most significant upstream regulators identified on the IPA pathway analysis (Figure 6).

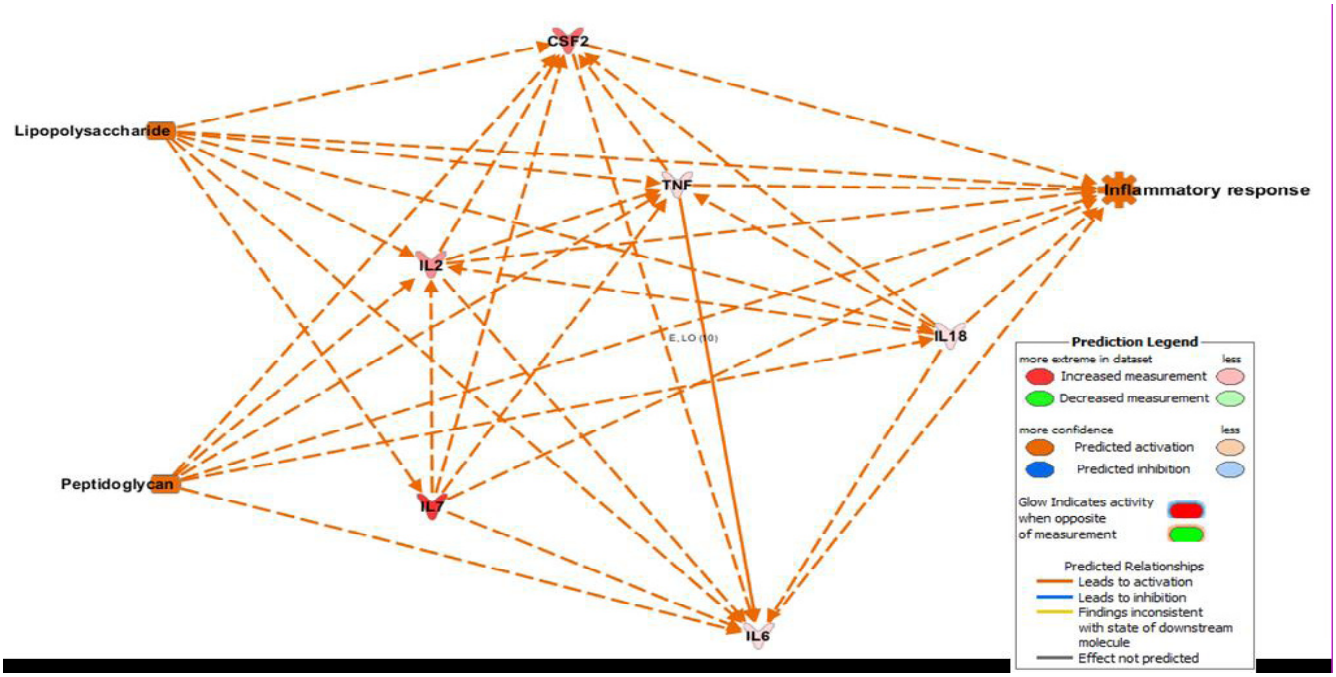

Figure 6: Prediction network showing the activation of pro-inflammatory biomarkers regulated by lipopolysaccharide and peptidoglycan (upstream regulators), leading to the activation of inflammatory response. The network shows the predicted interactions between IL-2, IL-6, IL-7, IL-18, CSF2 (or GM-CSF), TNFα, upstream regulators and infla mmatory responses at week 3 of EndoBarrier® implantation (N=7).

Discussion

This is the first study to show a significant and persistent systemic inflammatory response to the EndoBarrier®, and it is also the first to show alterations in the small intestinal microbiome following implantation of this device. In fact, the changes in the duodenal microbiome of our canine model by the time of EndoBarrier® removal were significant enough, and sufficiently similar to the normal fecal microbiome in control dogs, to suggest a 'Fecalization' had occurred in the microbiome of the small intestine during EndoBarrier® placement.

At the time of EndoBarrier® implantation, the canine duodenal microbiome was characterized by a high relative abundance of phylum Proteobacteria, followed in order of abundance by Bacteroidetes, Firmicutes and other phyla. By the time of EndoBarrier® explantation, this had shifted to a profile characterized by higher abundance of phylum Fusobacteria, followed by Firmicutes and Bacteroidetes. In comparison, the fecal microbiome of control dogs was characterized by higher abundances of Firmicutes, Bacteroidetes and Fusobacteria. Moreover, the phylum Firmicutes in the duodenum at explantation had shifted to a profile closer to that observed in the control fecal microbiome, which was characterized by high levels of the families Lactobacillaceae and Clostridiaceae. We hypothesize that these changes are the result of an increasingly anaerobic environment in the small intestine during EndoBarrier® placement, which allows for selection of obligate and facultative anerobic organisms that thrive in this environment, such as *Lactobacillus* and *Clostridium*. This hypothesis is supported by the significant reduction in family Aerococcaceae (which is predominantly aerobic), in the duodenum after EndoBarrier® placement.

While the profile of the duodenal microbiome did shift towards that of the normal fecal microbiome following Endobarrier® placement, there were also some distinct differences. For example, family Desulfovibrionaceae (phylum Proteobacteria, also predominantly anerobic) was increased the duodenal microbiome of dogs that underwent EndoBarrier® placement when compared to the normal canine fecal microbiome, in which this family was noticeably absent. It should be noted that Desulfovibrionaceae are sulfate reducers, and have been associated with inflammatory bowel disease [30-33]. There have also been reports of species within this family causing liver abscesses [34-37], which is interesting as liver abscesses were reported in human subjects who underwent Endobarrier® placement [7].

While the changes identified in the duodenal microbial profiles following EndoBarrier® placement are dramatic, the question remains as to whether the systemic inflammation observed (as demonstrated by the changes in cytokine and chemokine levels) is directly related to the alterations in the small bowel microbiome. Given that the EndoBarrier® is held in place in the duodenum by a nitinol anchor, it is possible that the increased levels of inflammatory markers identified are the direct result of irritation due to the device. In a previous published study, inflammatory markers in obese patients who had elevated baseline levels of inflammation were shown to be further increased after 3 months of EndoBarrier® placement [38]. While most markers of inflammation that were elevated in our study returned to baseline, levels of IL2 and GM-CSF remained elevated 6 weeks after EndoBarrier® removal, which could reflect a long-term change in the duodenal microbiome resulting from EndoBarrier® placement. Moreover, we note that the results of the IPA analysis suggest that the upstream regulators of these elevations in cytokine and chemokine levels included bacterial lipopolysaccharide and peptidoglycan. These findings support the possibility that the inflammation observed was related to the changes in the duodenal microbiome following placement of the Endobarrier®.

This study does have limitations. The sample size is small, although the analyses were performed using paired tests, which adds statistical power to the results. We did not collect stool from the Endobarrier®-implanted dogs, but rather from a control group of animals who were housed under the same conditions, as this allowed us to compare the changes in the duodenal microbiome following Endobarrier® placement to the normal fecal microbiome. Although this study was performed using a canine model, these findings have relevance for humans. Dogs are a good model of human obesity, as they gain weight in a manner that is comparable to humans when fed a diet similar to the Western diet. In contrast, most rodent models of obesity mimic the more severe, morbid obesity much less common among humans. Dogs are also an ideal model of diabetes and altered glucose metabolism, and the size of the duodenum in these animals is comparable to that humans, such that the Endobarrier® fit similarly.

Conclusion

While there is little doubt that adding a barrier between nutrient intake and the absorptive surface of the small bowel, as occurs with the EndoBarrier®, will result in weight loss and improved glycemic profile [5], questions have arisen as to the safety and tolerability of such a device. Our findings represent the first in-depth analysis of the effects of the EndoBarrier® on the small intestinal microbiome, and reveal an unhealthy pattern of microbial shifts consistent with the overgrowth of obligate and facultative anaerobes, coupled with inflammatory perturbations that persist beyond the removal of the device. We also show that the microbial shifts that occur include the growth of organisms associated with hepatic abscesses. These findings should be considered as the EndoBarrier® and other DJBL devices are further evaluated for clinical use in humans.

Acknowledgements

This study was supported in part by grants from the Monica Lester Charitable Trust and the Atol Charitable Trust to Dr. Ruchi Mathur. The funders played no roles in the study design, analysis or interpretation of the data, or in the preparation of the manuscript.

References

1. 2017a. IDF Diabetes Atlas, 8th edition. Brussels, Belgium: International Diabetes Federation.
2. 2017b. WHO | Diabetes. In WHO. World Health Organization.
3. 2018. WHO | Obesity and overweight. In WHO. World Health Organization.
4. Lemus R, Karni D, Hong D, Gmora S, Breau R, et al. (2018) The impact of bariatric surgery on insulin-treated type 2 diabetes patients. Surg Endosc 32: 990-1001.
5. Ruban A, Ashrafian H, Teare JP (2018) The EndoBarrier: Duodenal-Jejunal Bypass Liner for Diabetes and Weight Loss. Gastroenterol Res Pract 2018: 7823182.
6. Schouten R, Rijs CS, Bouvy ND, Hameeteman W, Koek GH, et al. (2010) A multicenter, randomized efficacy study of the EndoBarrier Gastrointestinal Liner for presurgical weight loss prior to bariatric surgery. Ann Surg 251: 236-243.
7. Glaysher MA, Mohanaruban A, Prechtl CG, Goldstone AP, Miras AD, et al. (2017) A randomised controlled trial of a duodenal-jejunal bypass sleeve device (EndoBarrier) compared with standard medical therapy for the management of obese subjects with type 2 diabetes mellitus. BMJ Open 7: e018598.
8. Ley RE, Bäckhed F, Turnbaugh P, Lozupone CA, Knight RD, et al. (2005) Obesity alters gut microbial ecology. Proceedings of the National Academy of Sciences of the United States of America 102: 11070-11075.
9. Ley RE, Turnbaugh PJ, Klein S, Gordon JI (2006) Human gut microbes associated with obesity. Nature 444: 1022.
10. Turnbaugh PJ, Ley RE, Mahowald MA, Magrini V, Mardis ER, et al. (2006) An obesity-associated gut microbiome with increased capacity for energy harvest. Nature 444: 1027.
11. Jumpertz R, Le DS, Turnbaugh PJ, Trinidad C, Bogardus C, et al. (2011) Energy-balance studies reveal associations between gut microbes, caloric load, and nutrient absorption in humans. The American Journal of Clinical Nutrition 94: 58-65.
12. Turnbaugh PJ, Hamady M, Yatsunenko T, Cantarel BL, Duncan A, et al. (2008) A core gut microbiome in obese and lean twins. Nature 457: 480.
13. Fernandes J, Su W, Rahat-Rozenbloom S, Wolever TMS, Comelli EM (2014) Adiposity, gut microbiota and faecal short chain fatty acids are linked in adult humans. Nutrition & Diabetes 4: e121.
14. Andreas S, David T, Klaus S, Silvia B, Bos NA, et al. (2010) Microbiota and SCFA in Lean and Overweight Healthy Subjects. Obesity 18: 190-195.
15. Gao R, Zhu C, Li H, Yin M, Pan C, et al. (2018) Dysbiosis Signatures of Gut Microbiota Along the Sequence from Healthy, Young Patients to Those with Overweight and Obesity. Obesity 26: 351-361.
16. Allin KH, Tremaroli V, Caesar R, Jensen BAH, Damgaard MTF, et al. (2018) Aberrant intestinal microbiota in individuals with prediabetes. Diabetologia 61: 810-820.
17. Hippe B, Remely M, Aumueller E, Pointner A, Magnet U, et al. (2016) Faecalibacterium prausnitzii phylotypes in type two diabetic, obese and lean control subjects. Beneficial Microbes 7: 511-517.
18. de Jonge C, Fuentes S, Zoetendal EG, Bouvy ND, Nelissen R, et al. (2019) Metabolic improvement in obese patients after duodenal-jejunal exclusion is associated with intestinal microbiota composition changes. Int J Obes (Lond) 43: 2509-2517.
19. Gill SR, Pop M, Deboy RT, Eckburg PB, Turnbaugh PJ, et al. (2006) Metagenomic analysis of the human distal gut microbiome. Science 312: 1355-1359.
20. Hooper LV, Midtvedt T, Gordon JI (2002) How host-microbial interactions shape the nutrient environment of the mammalian intestine. Annu Rev Nutr 22: 283-307.
21. Backhed F, Ding H, Wang T, Hooper LV, Koh GY, et al. (2004) The gut microbiota as an environmental factor that regulates fat storage. Proc Natl Acad Sci U S A 101: 15718-15723.
22. Ridlon JM, Kang DJ, Hylemon PB (2006) Bile salt biotransformations by human intestinal bacteria. J Lipid Res 47: 241-259.
23. Paszkiewicz RL, Burch MA, Bediako IA, Mkyrtchan H, Piccinini F, et al. 2018a. Impairing absorption of nutrients in the small intestine of normal weight, normoglycemic canines transiently impairs glucose effectiveness. In The Obesity Society meeting. New Orleans, LA.
24. Paszkiewicz RL, Burch MA, Bediako IA, Mkyrtchan H, Piccinini F, et al. 2018b. Increases in total bile acids drives metabolic changes in a non-obese canine model of reduced intestinal nutrient absorption. In The Obesity Society meeting New Orleans, LA.
25. Gersin KS, Keller JE, Stefanidis D, Simms CS, Abraham DD, et al. (2007) Duodenal- jejunal bypass sleeve: a totally endoscopic device for the treatment of morbid obesity. Surg Innov 14: 275-278.
26. Leite G, Morales W, Weitsman S, Celly S, Parodi G, et al. (2019) Optimizing Microbiome Sequencing for Small Intestinal Aspirates: Validation of Novel Techniques through the REIMAGINE Study. BMC Microbiol 19.
27. Klindworth A, Pruesse E, Schweer T, Peplies J, Quast C, et al. (2013) Evaluation of general 16S ribosomal RNA gene PCR primers for classical and next-generation sequencing-based diversity studies. Nucleic Acids Res 41: e1.
28. Quail MA, Swerdlow H, Turner DJ (2009) Improved protocols for the illumina genome analyzer sequencing system. Curr Protoc Hum Genet 8: 2.
29. Willis CR, Seamons A, Maxwell J, Treuting PM, Nelson L, et al. (2012) Interleukin-7 receptor blockade suppresses adaptive and innate inflammatory responses in experimental colitis. J Inflamm (Lond) 9: 39.
30. Muyzer G, Stams AJ (2008) The ecology and biotechnology of sulphate-reducing bacteria. Nat Rev Microbiol 6: 441-454.

31. Devkota S, Wang Y, Musch MW, Leone V, Fehlner-Peach H, et al. (2012) Dietary-fat-induced taurocholic acid promotes pathobiont expansion and colitis in Il10-/- mice. Nature 487: 104-108.

32. Rowan F, Docherty NG, Murphy M, Murphy B, Calvin Coffey J, et al. (2010) Desulfovibrio bacterial species are increased in ulcerative colitis. Dis Colon Rectum 53: 1530-1536.

33. Nagao-Kitamoto H, Kamada N (2017) Host-microbial Cross-talk in Inflammatory Bowel Disease. Immune Netw 17: 1-12.

34. Tee W, Dyall-Smith M, Woods W, Eisen D (1996) Probable new species of Desulfovibrio isolated from a pyogenic liver abscess. J Clin Microbiol 34: 1760-1764.

35. Yamazaki T, Joshita S, Kasuga E, Horiuchi K, Sugiura A, et al. (2018) A case of liver abscess co-infected with Desulfovibrio desulfuricans and Escherichia coli and review of the literature. J Infect Chemother 24: 393-397.

36. Koyano S, Tatsuno K, Okazaki M, Ohkusu K, Sasaki T, et al. (2015) A Case of Liver Abscess with Desulfovibrio desulfuricans Bacteremia. Case Rep Infect Dis 2015: 354168.

37. Hagiya H, Kimura K, Nishi I, Tomono K (2018) Liver abscess caused by Gram-negative spiral bacilli. JMM Case Rep 5: e005155.

38. de Jonge C, Rensen SS, D'Agnolo HM, Bouvy ND, Buurman WA, et al. (2014) Six months of treatment with the endoscopic duodenal-jejunal bypass liner does not lead to decreased systemic inflammation in obese patients with type 2 diabetes. Obes Surg 24: 337-341.